JOURNAL OF MATERIALS SCIENCE 13 (1978) 1855–1867

Some physical properties of V_2O_5-Fe_2O_3 and V_2O_5-Fe_2O_3-Li_2O systems

E. BURZO, L. STĂNESCU, V. TEODORESCU,
National Center of Physics, P.O. Box 5206, Bucharest, Romania
I. ARDELEAN, M. COLDEA
Faculty of Physics, University of Cluj-Napoca, Romania

Various methods have been used to study the physical properties of the $V_2O_5-Fe_2O_3$ and $V_2O_5-Fe_2O_3-Li_2O$ systems, including X-ray, electron microscope, Mössbauer effect, NMR and thermogravimetric measurements. The iron ions are approximately equally distributed in substitutional and interstitial sites in the V_2O_5 lattice. The maximum number of iron ions dissolved in the V_2O_5 matrix corresponds to 4 mol % Fe_2O_3. In all the samples a quantity of Fe_2O_3 which has not been included in lattice is observed. The $V_2O_5-Fe_2O_3$ and $V_2O_5-Fe_2O_3-Li_2O$ systems are formed from solid solutions mixed with very small Fe_2O_3 particles. The analysis of the charge compensation of iron ions suggests that V_2O_5 is a quasi-amorphous semiconductor. Irradiation of V_2O_5-based samples with an electron beam induces the V_2O_5 platelets to convert to the VO_x phase.

1. Introduction

Vanadium pentoxide crystallizes in the orthorombic-type structure; space group Pmnm [7]. The vanadium ions are surrounded by five oxygen ions making a trigonal bipyramid (Fig. 1). The pyramids are arranged in layers in the *a–c* plane. In the layers, the binding forces between V–O–V chains are of both covalent and ionic type. The V=O bonds in the plane perpendicular to the *a–c* plane are of vanadyl-type while the binding forces between planes are of Van der Waals-type.

Pure stoichiometric V_2O_5 should be an isolator, but non-stoichiometric [2] or doped [3] V_2O_5 is known to be a low mobility n-type semiconductor. The doped ions may occupy interstitial or substitutional sites in the V_2O_5 lattice. For example the vanadium ions may substitute for T^{6+} (T = Mo, W) [4], while the monovalent ions such as Na^+, Li^+, Cu^+ etc. occupy interstitial sites [5]. The electronic properties of these systems are attributed generally to the presence of V^{4+} ions, resulting from charge compensation of the doping ions by valence induction.

Using Mössbauer effect studies, Abdullaev *et al.* [6], have demonstrated that Fe^{3+} ions may occupy

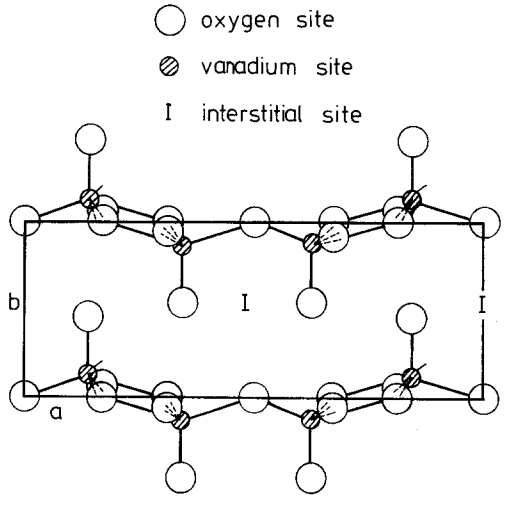

Figure 1 The V_2O_5 crystalline structure.

both substitutional and interstitial sites in the V_2O_5 lattice (Fig. 1). By ESR measurements, Jansen and Sperlich [7] showed that the relative occupation numbers of both sites are not proportional to the initial Fe_2O_3 content. They conclude that this behaviour is either caused by other valency states of the iron ions, or the sub-

stitution of Fe^{3+} ions is not proportional to the iron concentration in the melt. Analysing the charge compensation of iron ions in the V_2O_5 lattice, they conclude that this is mainly self-compensation. The self-compensating system is formed by the Fe^{3+}–$V_{O^{2-}}$ complex, involving the lack of one oxygen ion. At higher iron concentrations the number of V^{4+} ions decreases; one possibility may be described by $Na_x^+ V_{2-x}^{5+} V_{x-y}^{4+} Fe_y^{4+} O_5^{2-}$. The ESR spectra, however, do not reveal if there are other valency states of iron ions and is they are responsible for the observed decrease in the number of V^{4+} ions.

In order to determine the range of solubility of the iron ions in the V_2O_5 lattice and also to analyse the problem of charge compensation of iron ions, we have studied the V_2O_5–Fe_2O_3 and V_2O_5–Fe_2O_3–Li_2O systems, using X-ray analysis, electron microscope studies, Mössbauer effect and NMR measurements, as well as thermogravimetric analysis. Some preliminary results concerning the Mössbauer effect measurements on the V_2O_5–Fe_2O_3 system have already been published [8].

In order to analyse the influence of the monovalent ions on the compensation of charge differences introduced by Fe^{3+} ions in the V_2O_5 lattice, Li^+ was used. Li_2O forms solid solutions with V_2O_5, up to 6.5 mol% Li_2O, while the solubility of Na_2O is limited to 1 mol% [5].

2. Experimental

The pure constituents were mixed together, powdered and then melted at 800° C in a platinum crucible. Two sets of samples were then obtained. In the first case the alloys were quenched from the liquid state, in order to preserve the greater quantity of iron ions in the V_2O_5 lattice. Some samples were also prepared by cooling the melt very slowly, in order to induce – if possible – the charge compensation, transition of the iron ions from the Fe^{3+} state to the Fe^{4+} one, respectively.

The X-ray analyses were made with a Seifert-type equipment. The diffraction lines were obtained using CuKα radiation. The diffraction patterns show only the lines characteristic of the V_2O_5 structure for all the samples. The intensities of the lines are different from those on non-doped V_2O_5.

The lattice parameters of the V_2O_5–Fe_2O_3 and V_2O_5–Fe_2O_3–Li_2O samples are given in Table I. The introduction of iron ions into the V_2O_5 matrix leads to the modification of lattice parameters. These variations seem to be rather small. The presence of lithium ions increases the *a* and *b* lattice parameters, while *c* remains unchanged. It is to be noted that in all cases only one phase is observed. The electron microscope patterns and electron diffraction study were made with a JEM-120 electron microscope.

TABLE I Lattice parameters of V_2O_5–Fe_2O_3 and V_2O_5–Fe_2O_3–Li_2O solid solutions

Sample composition (mol%)		Lattice parameters (Å)		
Fe_2O_3	Li_2O	*a*	*b*	*c*
1	–	11.480	4.360	3.556
2	–	11.460	4.350	3.544
2.5	–	11.457	4.341	3.539
2.5	2.5	11.471	4.350	3.541
2.5	5	11.475	4.357	3.540
3	–	11.452	4.340	3.538
4	–	11.415	4.335	3.520
4	2.5	11.448	4.352	3.522
5	–	11.400	4.325	3.512
15	–	11.510	4.358	3.555

The Mössbauer effect measurements were performed with an ELRON and ASA-type equipment at 78 K and 295 K. A Co^{57} source in a copper matrix was used. The experimental spectra were analysed using a FORTRAN program assuming a Lorentzian shape of the lines [9]. Using such a program we can determine the integrated area under the absorption lines and consequently the relative content of iron ions with different coordination or valence states.

The NMR spectra of V^{51} in powdered V_2O_5–Fe_2O_3 samples were recorded at 9.212 MHz, using a JNM-3 spectrometer improved by a broad-line attachment, JNM-BH-2, at room temperature. The thermal analyses were performed using an ORION-GYEM derivatograph.

3. Mössbauer effect measurements

3.1. The V_2O_5–Fe_2O_3 system

The Mössbauer spectra obtained at $T = 295$ and 78 K for the sample with initial Fe_2O_3 content, $x = 15$ mol% Fe_2O_3, are shown in Fig. 2. The spectra obtained in the case of samples with a lower iron content ($x = 2.5$ and 4 mol% Fe_2O_3) are shown in Figs. 6 and 7. No hyperfine splittings are observed over the studied concentration range ($x \leqslant 15$ mol% Fe_2O_3) in the temperature range $T \geqslant 78$ K.

The spectra consist of three doublets, in

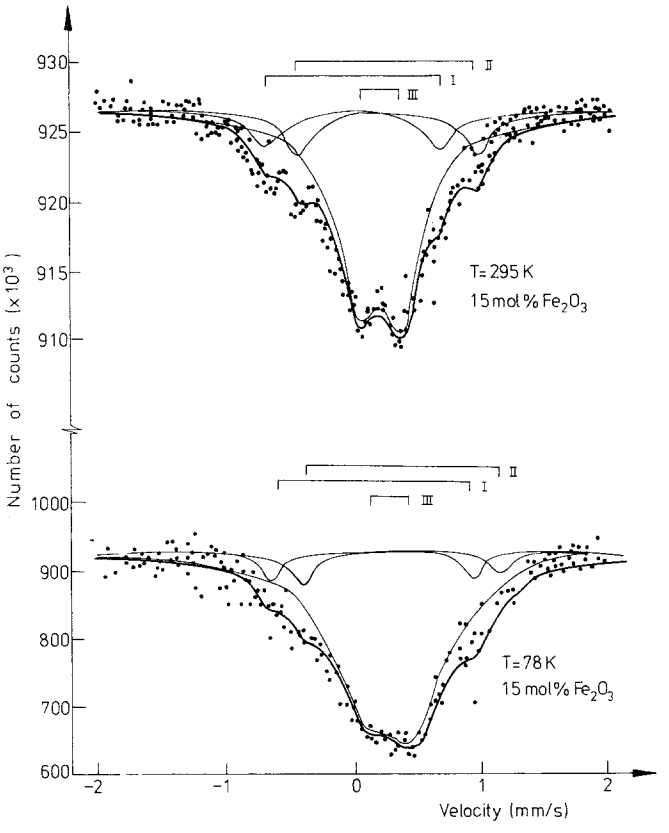

Figure 2 The Mössbauer spectra of V_2O_5 + 15 mol% Fe_2O_3 samples at 295 and 78 K. The calculated doublets are represented by solid lines.

agreement with the results of Abdullaev *et al.* [6]. The antisymmetric doublet denoted by III is attributed to Fe_2O_3 particles which have not been included in V_2O_5 lattice. The doublets I and II are attributed to the iron ions which substitute for vanadium ions and occupy interstitial sites, respectively.

The isomer shift values, δ, can be used to decide which doublets are due to the interstitial and substitutional sites. The composition dependence of the isomer shift is shown in Fig. 3. According to the diagram by Walker *et al.* [10] the iron ions which contribute to the doublets II have nearly ionic bonds and consequently are attributed to Fe^{3+} ions in interstitial sites. The doublets I are evidence of covalent bounding. These are attributed to the iron ions which substitute for the vanadium ones. The δ_I and δ_{II} values increase slightly with increase in iron content. The isomer shift, δ_{III}, characterizing the Fe_2O_3 particles not included in the V_2O_5 lattice is composition independent.

In Fig. 4 we show the composition dependence of the quadrupole interaction, ΔQ. The ΔQ values characteristic of the doublets I and II increase with the iron content in the lattice. This is the result of

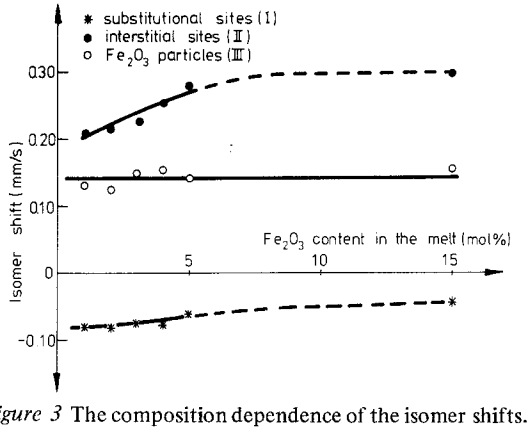

Figure 3 The composition dependence of the isomer shifts.

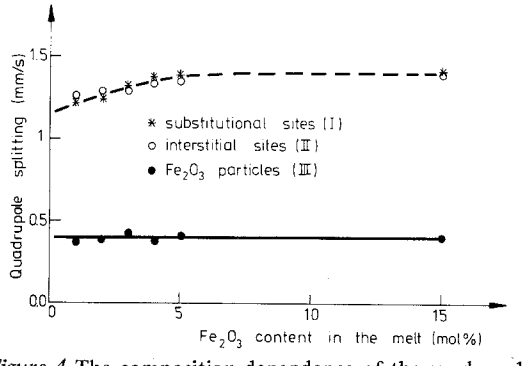

Figure 4 The composition dependence of the quadrupole splittings.

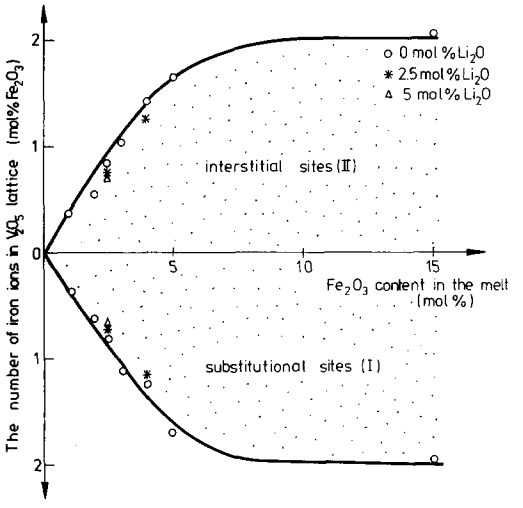

Figure 5 The number of iron ions dissolved in the V_2O_5 lattice as a function of the initial Fe_2O_3 content. The values obtained for some samples with Li_2O are also plotted.

the deformation of the V_2O_5 lattice, caused by the incorporation of an increasing number of iron ions. For a given concentration, the quadrupole splitting is nearly the same for the iron ions in both substitutional and interstitial sites. The quadrupole interaction characterizing the doublet III is not dependent on composition.

From the integrated areas under the absorption curves we can determine the iron content in the V_2O_5 lattice in various environments. The results are shown in Fig. 5. The iron content in the V_2O_5 lattice seems to increase nearly linearly with initial Fe_2O_3 content, up to 4 mol % Fe_2O_3, and then tends asymptotically to a value which corresponds to 4 mol % Fe_2O_3, almost equally distributed between interstitial and substitutional sites.

In all the samples studied, in addition to the iron ions present in the V_2O_5. lattice, there is evidence of a certain number of Fe_2O_3 particles. No hyperfine splittings have been observed even at 78 K, in spite of the high iron content. This is a consequence of the very small dimensions of these particles. Suzdalev [11] has studied the correlation between the values of T_c, transition temperatures, for the transformation from the paramagnetic to the antiferromagnetic state, and the volume of these particles. This shows that the critical volume, V_{cr}, depends linearly on the temperature, T_c:

$$V_{cr} \simeq 4 \times 10^{-2} T_c \qquad (1)$$

where V_{cr} is given in cm^3 and T_c in K.

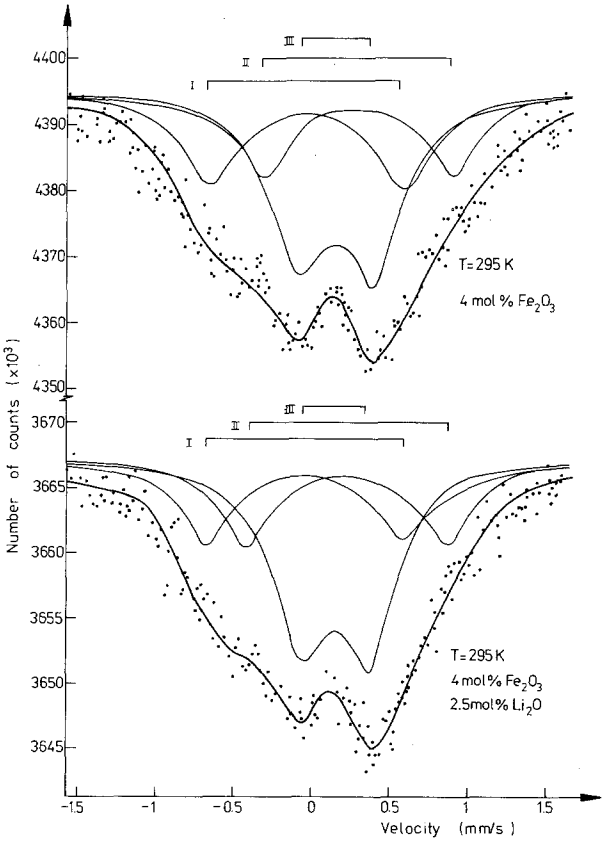

Figure 6 The Mössbauer spectra of the samples with 4 mol % Fe_2O_3 and $y = 0$ and 2.5 mol % Li_2O.

For $V < V_{cr}$, the Fe_2O_3 particles are superparamagnetic, while for $V > V_{cr}$ they have an antiferromagnetic order.

Using Relation 1 and considering that the Fe_2O_3 particles are superparamagnetic at 78 K, we conclude that their dimensions are smaller than 60 Å.

3.2. The $V_2O_5-Fe_2O_3-Li_2O$ system

In order to analyse the mechanism of charge compensation of iron ions in the V_2O_5 lattice, we studied some ternary $V_2O_5-Fe_2O_3-Li_2O$ alloys, with variable lithium content, keeping the Fe_2O_3 concentration constant at 2.5 and 4 mol%, respectively.

The Mössbauer spectra of the samples with 4 mol% Fe_2O_3 and with and without 2.5 mol% Li_2O are shown in Fig. 6. In Fig. 7 the spectra of the alloys with 2.5 mol% Fe_2O_3 and 0, 2.5 and 5 mol% Li_2O, respectively, are plotted. As seen from these figures the form of the spectra is similar both with and without Li_2O.

The dependence of the number of iron ions in the V_2O_5 lattice, as function of Li_2O content is given in Fig. 5. In the samples containing lithium, the iron content is somewhat smaller than that determined in samples with identical Fe_2O_3 content but without Li_2O.

The dependence of the isomer shifts and quadrupole splittings, as a function of Li_2O content, is shown in Figs. 8 and 9. No discernible differences are observed within the limit of experimental error.

We do not notice valency states of iron ions other than Fe^{3+}, induced by the presence of lithium. Consequently, in case of a high iron content, we cannot observe the compensating mechanism, as previously suggested [7].

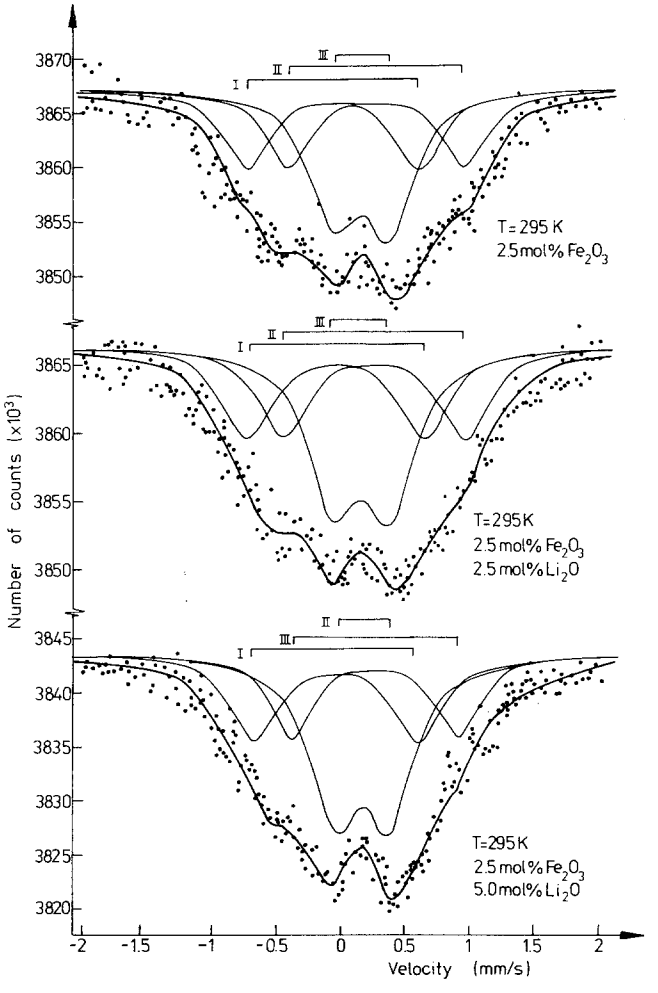

Figure 7 The Mössbauer spectra of the samples with 2.5 mol% Fe_2O_3 and $y = 0$, 2.5 and 5.0 mol% Li_2O.

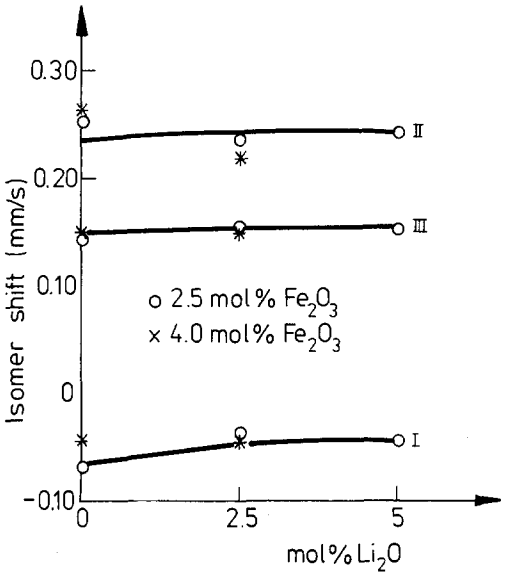

Figure 8 The dependence of the isomer shifts on Li_2O content.

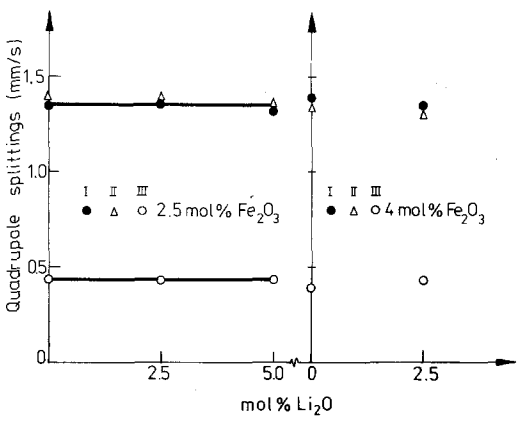

Figure 9 The dependence of quadrupole splittings on Li_2O content.

4. Nuclear magnetic resonance (NMR) study of the $V_2O_5 - Fe_2O_3$ system

By NMR measurements we analysed the deformation of the V_2O_5 lattice, as result of the introduction of iron ions. The NMR absorption lines for the samples with 1 and 5 mol % Fe_2O_3 are shown in Fig. 10. For the samples with 1 mol % Fe_2O_3 we observe only four satellite lines, equally spaced on each side on the main nuclear resonance line. This is due to a poor resolution of the spectra. For the sample with 5 mol % Fe_2O_3 only the central line is observed. This is the result of the second order quadrupole effects [12, 13].

The resonance frequencies for the case of small quadrupole interaction, a nucleus of spin $I = 7/2$, and axial symmetry for the electric field gradient

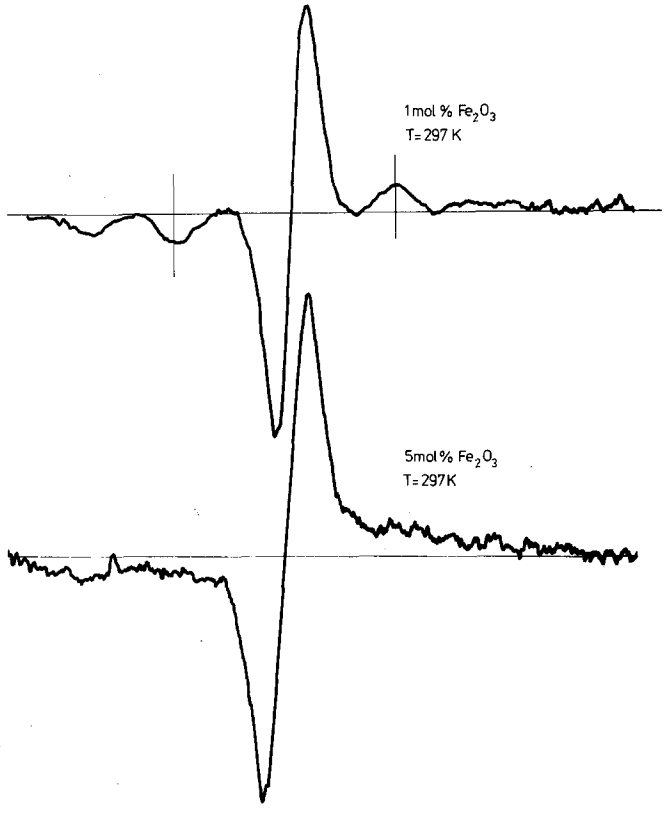

Figure 10 The V^{51} nuclear absorption spectra in V_2O_5 with 1 mol % Fe_2O_3 and 5 mol % Fe_2O_3.

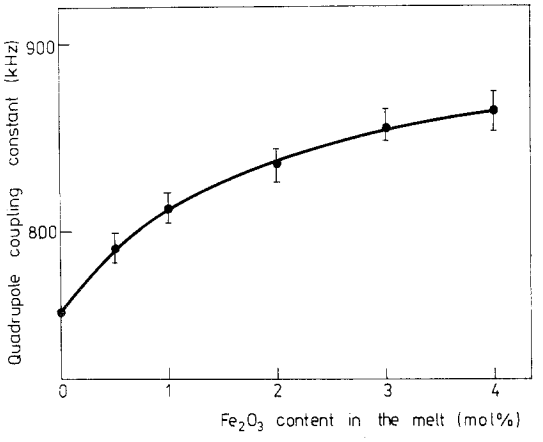

Figure 11 The dependence of the quadrupole coupling constant on initial Fe_2O_3 content.

is given by:

$$\nu_{m \to m-1} = \nu_0 + (2m-1)\frac{1}{56}\frac{e^2qQ}{h} \quad (2)$$

where e^2qQ/h is the quadrupole coupling constant, which is a measure of the electric field gradient at vanadium sites.

Since in the $V_2O_5-Fe_2O_3$ samples, the spectra do not show all the satellite lines, the quadrupole coupling constant was determined from the $m = 1/2 \to 3/2$ transition, corresponding to the first pair of satellite lines.

We show in Fig. 11 the dependence of the quadrupole coupling constants on the initial Fe_2O_3 content. The e^2qQ/h values increase with nominal Fe_2O_3 concentration. This is evidence of continuous deformation of the crystalline cell. These results confirm the Mössbauer effect data.

5. Thermogravimetric measurements

Thermogravimetric measurements may be used to determine the variation of the weight at the solidification temperature after lattice formation as result of the oxygen release. This method has been used to estimate the number of V^{4+} ions, due to the valence induction by W^{6+} or Mo^{6+} ions in the $V_2O_5-WO_3$ and $V_2O_5-MoO_3$ systems [14]. Thus thermogravimetric measurements may be used to verify the validity of the self-compensating mechanism, where there is a lack of an oxygen ion [7].

Fig. 12 shows some typical thermograms for the $V_2O_5-Fe_2O_3$, $V_2O_5-Fe_2O_3-Li_2O$, $V_2O_5-Li_2O$ and $V_2O_5-WO_3$ systems. The weight of all samples was 1 g. For the $V_2O_5-Fe_2O_3$ system (Fig. 12a) we did not observe a weight variation at

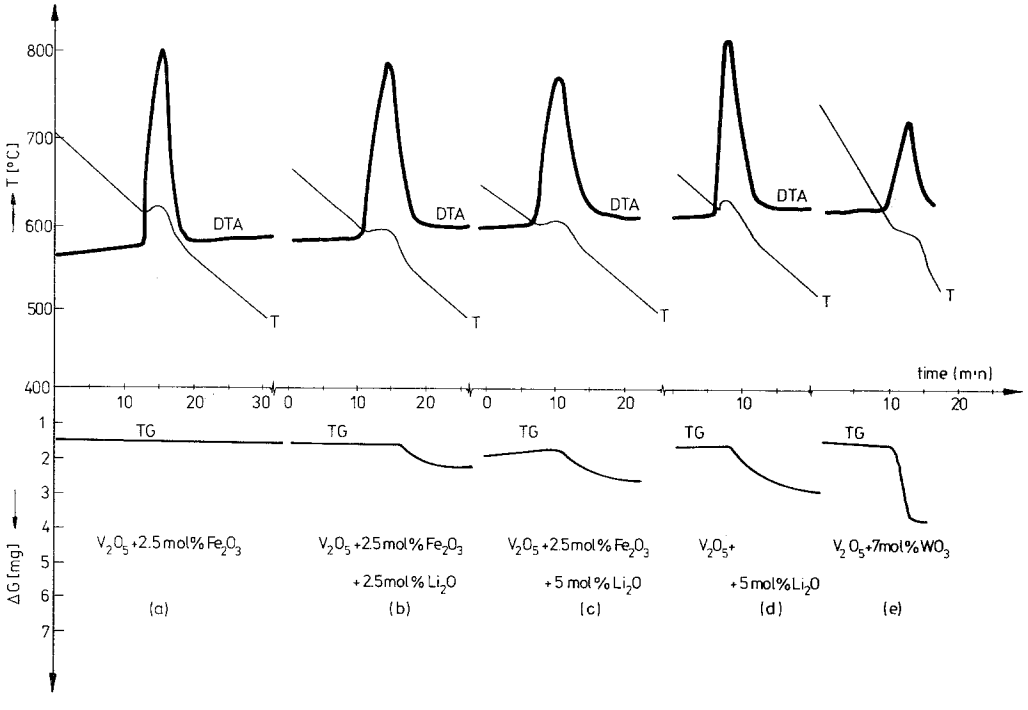

Figure 12 Typical thermograms for $V_2O_5-Fe_2O_3$, $V_2O_5-Fe_2O_3-Li_2O$, $V_2O_5-Li_2O$ and $V_2O_5-WO_3$ samples. Temperature is denoted by T, thermogravimetric analysis by DTA the weight of sample by TG and the relative variation of weight by ΔG.

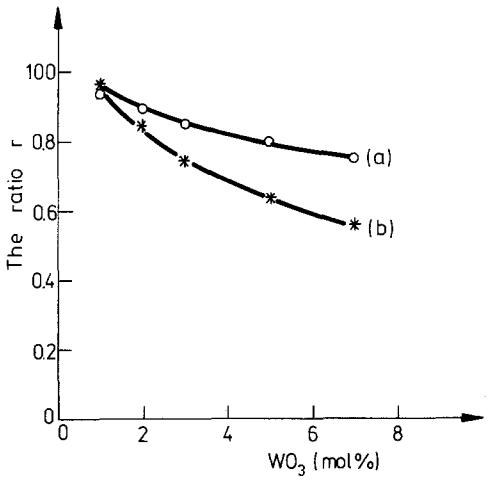

Figure 13 The number of V^{4+} ions induced by the presence of W^{6+} ions. (a) Using thermogravimetric data; (b) by magnetic measurements.

the solidification temperature. In this system, no evidence of oxygen release is observed. We conclude that the self-compensating mechanism, which requires the lack of an oxygen ion, is not confirmed. The degree of non-stoichiometry of V_2O_5 probably corresponds, in this case, to that

TABLE II The weight variation and ratio r of the number of V^{4+} ions to number of doping ions, determined from the thermograms of Fig. 12

Sample	Relative variation in weight (mg g^{-1})	r
V_2O_5 + 2.5 mol % Fe_2O_3	0	0
V_2O_5 + 2.5 mol % Fe_2O_3 + 2.5 mol % Li_2O	0.62	0.283
V_2O_5 + 2.5 mol % Fe_2O_3 + 5 mol % Li_2O	0.81	0.185
V_2O_5 + 5 mol % Li_2O	1.25	0.285
V_2O_5 + 7 mol % WO_3	2.19	0.75

of an undoped sample, being of the order of magnitude of experimental error.

As seen from Figs. 12b to d, a weight variation at the solidification temperature, due to oxygen release, is observed in the samples containing lithium. This is due to the induction of V^{4+} ions by lithium ones. The ratio r of the number of V^{4+} ions to that of Li^+ ions is less than one, suggesting an incomplete compensation of their charge differences (Table II).

In the V_2O_5–WO_3 solid solutions we have determined the number of oxygen and V^{4+} ions

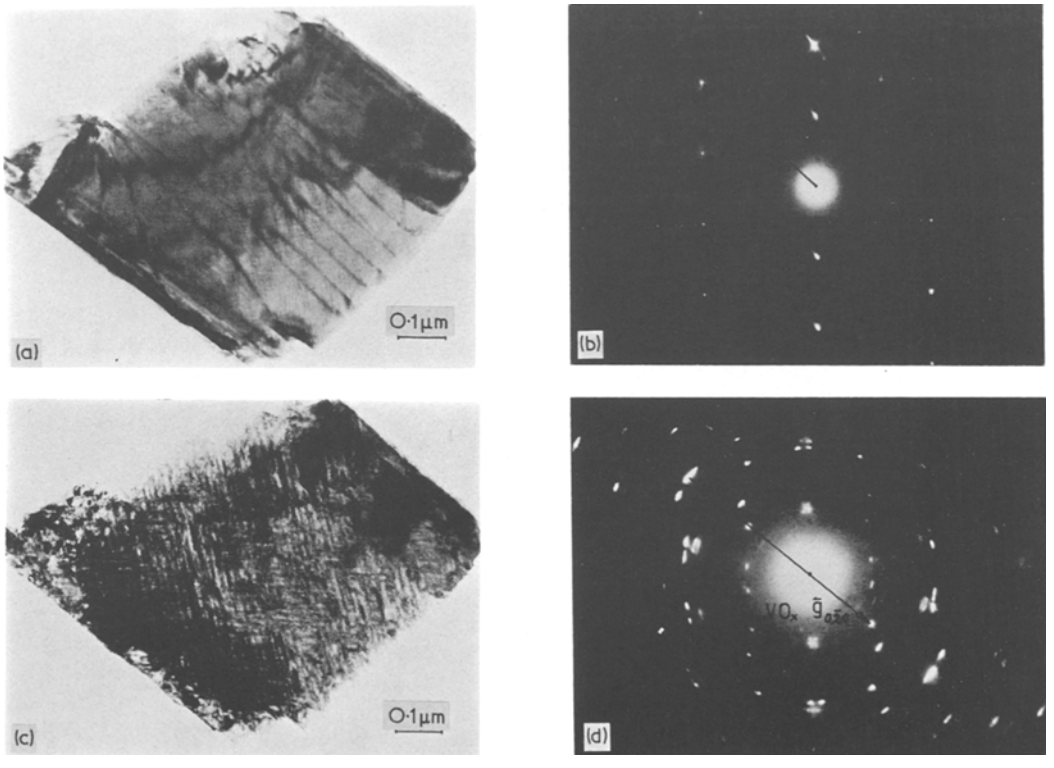

Figure 14 The electron microscope image (a) and electron diffraction pattern (b) for a V_2O_5 sample at the start of the irradiation in the microscope and (c) and (d) after irradiation by the electron beam in the microscope.

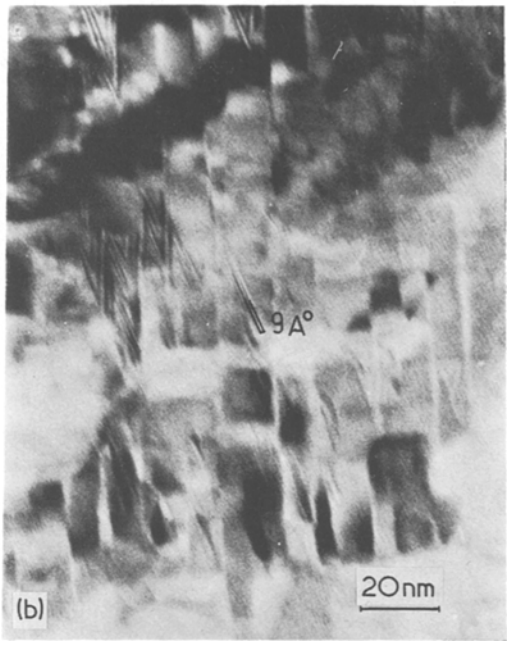

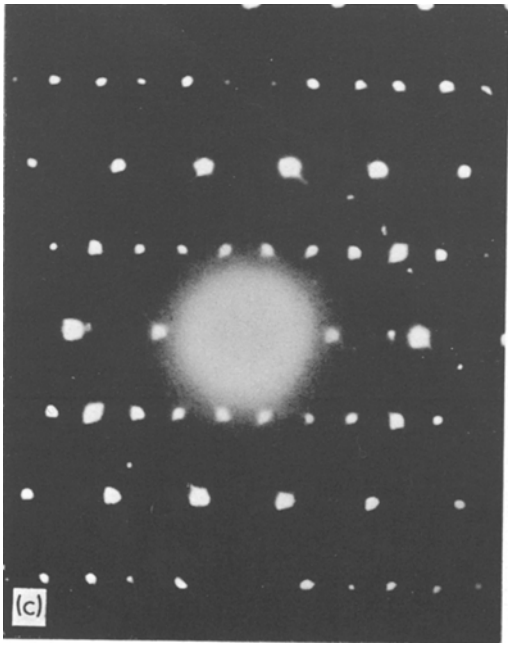

Figure 15 The mosaic structure of the V_2O_5 + 1 mol% Fe_2O_3 sample (a). (b) The same image much enlarged and (c) the electron diffraction pattern.

which are missing from the stoichiometric V_2O_5 matrix, respectively (Fig. 12e). The composition dependence of the ratio of the number of V^{4+} ions to W^{6+} ions is given in Fig. 13. On the same figure is plotted the composition dependence of the same ratio, using the number of V^{4+} ions determined by magnetic measurements [15]. The agreement between these two sets of data is satisfying, though two different methods are used, thus confirming the validity of the results of thermogravimetric measurements.

6. Electron microscope study

The powdered samples were mixed with a colodium solution and then laid on a glass plate in the form of thin films. The colodium films were then taken out and fixed on the grill. The crystallites generally have the (0 0 1) plane parallel to the colodium film. The common form of the V_2O_5 powders is thin platelets.

In order to analyse the influence of the preparation conditions, we studied pure V_2O_5 samples both slowly cooled and also quenched from the melt. We did not observe any difference between the distribution of the crystallites in these samples. The common dimension of both slowly cooled samples and those quenched from the melt is 0.1 to 1 μm, but in the slowly cooled samples some crystallites have greater platelet dimensions of 10 to 100 μm.

Under the action of the electron beam in the microscope, the V_2O_5 platelets convert into the VO_x phase of unknown composition, formed by the reduction of V_2O_5. The VO_x structure is orthorombic with parameters $a_0 = 8.1$ Å, $b_0 = 10.4$ Å and $c_0 = 16.1$ Å [16, 17]. The electron

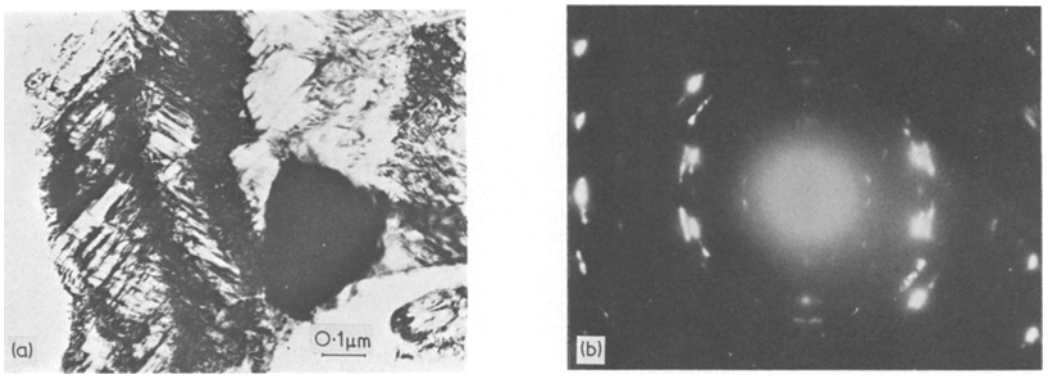

Figure 16 The electron microscope image of the sample with 5 mol % Fe_2O_3 (a); and the electron diffraction pattern (b).

diffraction patterns give evidence that the vector g_{310} of V_2O_5 coincides with the vector g_{040} of the VO_x structure.

As previously observed by the transformation of V_2O_5 to the VO_x structure, some twins appear in the crystallites with a (3 1 0) twinning plane. The first stage of this transformation is twinning, followed by the formation of the VO_x structure.

The V_2O_5 sample quenched from the melt at the beginning of irradiation is shown in Fig. 14. In the electron diffraction patterns only the maxima corresponding to the [0 0 1] direction of V_2O_5 crystallite appear (Fig. 14b). Fig. 14c shows the same crystallite after a long period of irradiation. In the electron diffraction patterns the V_2O_5 crystallite, the twins and the VO_x structure which is also twinned can be seen (Fig. 14d).

Figs. 15 to 17 show the electron microscope patterns of the V_2O_5 samples with initial Fe_2O_3 contents of 1, 5 and 15 mol % respectively. Fig. 15a, the V_2O_5 + 1 mol % Fe_2O_3 sample, shows the mosaic structure of the crystallites, and a much enlarged portion is shown in Fig. 15b. The electron diffraction pattern, Fig. 15c, shows the presence of the VO_x structure. In this case the crystallite is in the (0 0 1) plane. The characteristic appearance of a crystallite having 5 mol % Fe_2O_3 is shown in Fig. 16a, while the characteristic reflections of V_2O_5 and VO_x structures are shown in Fig. 16b.

The electron beam irradiation of the small crystallites ($< 0.1\,\mu m$) in the microscope induces transformations of the crystalline morphology, substantially modifying the electron diffraction image. This may be seen in Fig. 17a, where the image for the sample with 15 mol % Fe_2O_3 is shown. At the start of the electron microscope observation (irradiation), the crystallites have their initial form (Fig. 17b). After irradiation with a strong electron beam the transformation which takes place by recrystallization may be observed (Fig. 17c).

In the samples containing iron, the transformation from the V_2O_5 to the VO_x phase takes place less readily than in the pure V_2O_5 sample. Fig. 18 shows the electron microscope and electron diffraction patterns of the samples containing 2.5 mol % Fe_2O_3 with and without 5 mol % Li_2O. The images are nearly the same, showing only the lines characteristic of the V_2O_5 structure.

No Fe_2O_3 particles were identified in any of the samples, although Mössbauer effect measurements indicated that they were present. The Fe_2O_3 particles are probably disposed as molecular precipitates near the lattice defects and appear in contrast together with the VO_x phase.

The presence of the Fe_2O_3 phase has not been observed by electron diffraction, confirming the results of the Mössbauer effect study, with respect to their very small dimensions.

7. Discussion

The Fe^{3+} ions in the V_2O_5 lattice are approximately equally distributed between interstitial and substitutional sites. The number of iron ions in the V_2O_5 lattice is dependent on the initial Fe_2O_3 content, as shown in Fig. 5, and generally is not proportional to the Fe_2O_3 content in the melt. The V_2O_5–Fe_2O_3 system consists of a solid solution of iron in the V_2O_5 lattice, mixed with

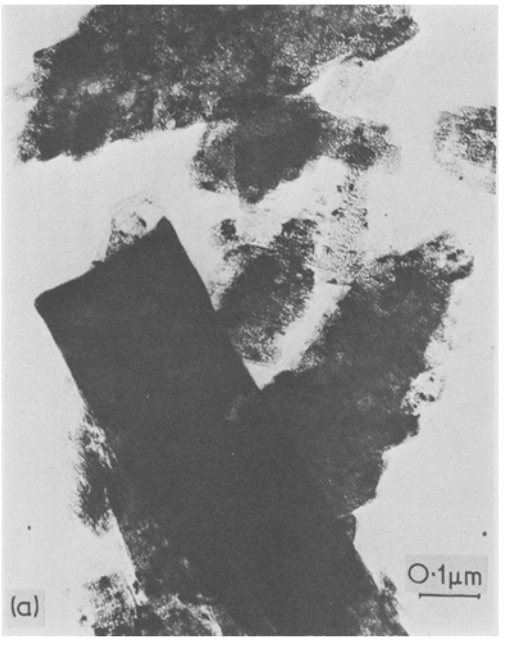

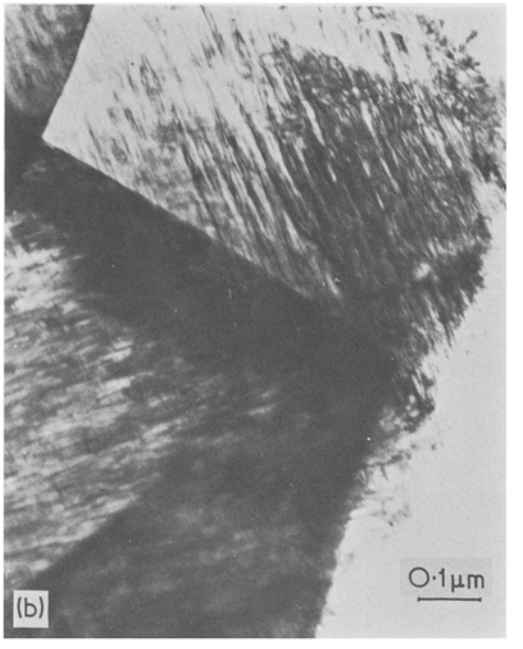

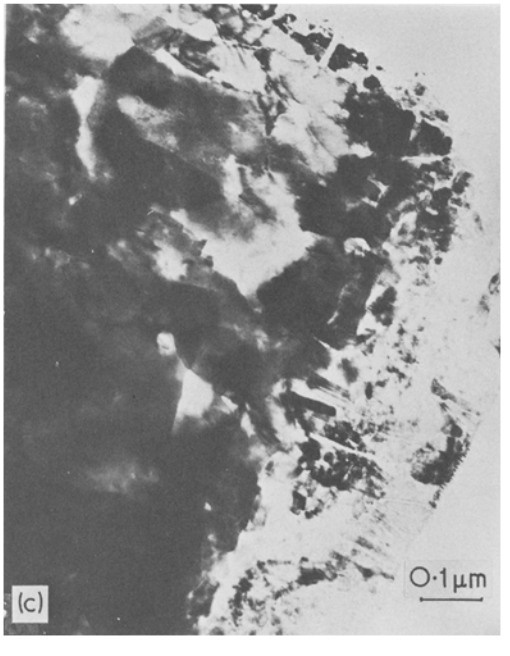

Figure 17 The electron microscope image of the sample with 15 mol% Fe_2O_3, (b) after a weak electron beam irradiation and (c) the same sample after strong electron beam irradiation.

small Fe_2O_3 particles not incorporated in the matrix. These particles seem to be about the same size as the crystalline cell and thus cannot be observed by either X-ray analysis or electron diffraction studies. It is probable that the Fe_2O_3 particles are present as molecular precipitates near the lattice defects and appear in contrast in the electron microscope, similar to the VO_x phase.

In the case of both quenched and slowly cooled samples, within the limit of experimental error, there are the same numbers of iron ions in the V_2O_5 lattice. This quantity is not influenced by the way in which the samples were prepared. The study of the $V_2O_5-Fe_2O_3-Li_2O$ system gives evidence that the number of iron ions in the lattice decreases slightly. In none of the samples did we notice valency states of iron ions other than Fe^{3+}. Thus, for a high iron content one cannot observe the previously suggested [7] compensating mechanism.

The thermogravimetric study does not show a lack of oxygen ions in the V_2O_5 lattice, and consequently the self-compensating mechanism involving the $Fe^{3+}-V_{O^{2-}}$ complex [7]. Thus, from the experimental data, it is difficult to imagine a model for the compensation of charge differences introduced by the iron ions. As previously suggested [8], the behaviour of the $V_2O_5-Fe_2O_3$ and $V_2O_5-Fe_2O_3-Li_2O$ systems may be explained, assuming V_2O_5 to be a quasi-amorphous semiconductor. In this case, no compensation of charge differences introduced by the iron ions is required [18, 19].

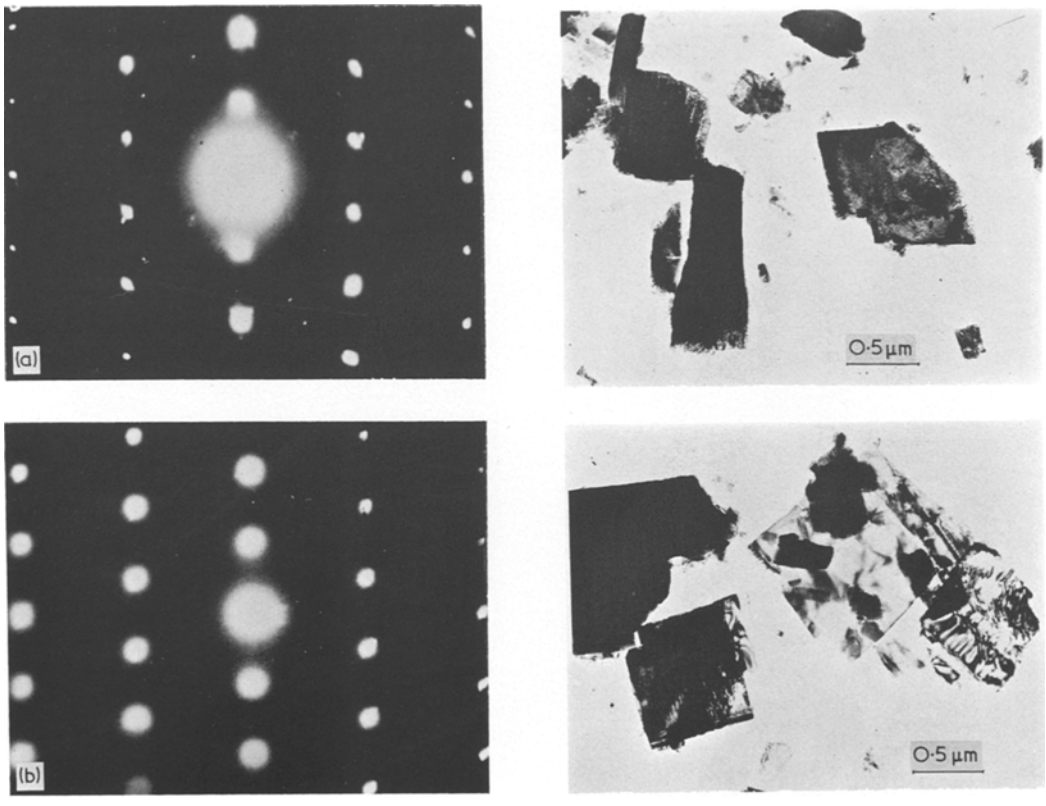

Figure 18 The electron microscope and electron diffraction patterns of the samples with 2.5 mol% Fe_2O_3 and (a) $y = 0$ mol% Li_2O; (b) $y = 2.5$ mol% Li_2O.

The quasi-amorphous behaviour of V_2O_5 was also suggested by electrical measurements of V_2O_5 single crystals [20] and the study of $V_2O_5-WO_3$ and $V_2O_5-MoO_3$ solid solutions [15, 21]. For example, in the last case the ratio between the number of V^{4+} ions and the doped T^{6+}(T = W or Mo) ions is less than one. Thus, in these solid solutions, not all the charge differences is compensated for.

As the iron content increases, the lattice is more deformed, as observed both by Mössbauer effect studies and NMR measurements.

The irradiation of V_2O_5-based samples with the electron beam in microscope induces the V_2O_5 platelets to convert to the VO_x phase. In the case of samples containing iron, this transformation takes place less readily than in pure V_2O_5.

References

1. L. V. DIMITRIEVA, V. A. IOFFE and I. B. PATRINA *Fiz. Tverd. Tela* 7 (1965) 2754.
2. V. A. IOFFE and I. B. PATRINA, *Phys. Stat Sol.* **40** (1970) 389.
3. E. GILLIS and E. BOESMAN, *ibid.* **14** (1966) 337.
4. V. A. IOFFE and I. B. PATRINA, *Fiz. Tverd. Tela* **10** (1968) 815.
5. P. HAGENMULLER, J. GALY, M. POUCHARD and A. CASALOT, *Mater. Res. Bull.* **1** (1966) 45.
6. A. S. ABBDULLAEV, L. M. BELYAEV, T. V. DIMITRIEVA, D. F. DOBRZHANSKI, V. V. HYUKHIN and I. S. LYUBUTIN, *Sov. Phys. Crystallogr.* **14** (1969) 389.
7. K. JANSEN and G. SPERLICH, *Phys. Stat Sol. (b)* **55** (1973) 495.
8. E. BURZO and E. STĂNESCU, *Sol. Stat. Comm.* **20** (1976) 653.
9. D. P. LAZAR and M. MORARIU, Preprint IFA SR. 17 (1976).
10. L. R. WALKER, G. K. WERTHEIM and V. JACCARINO, *Phys. Rev. Lett.* **6** (1961) 98.
11. I. P. SUZDALEV, Proceedings of the Conference on the Application of Mössbauer effect, Tihany (1969) p.13.
12. D. E. O' REILLY, *J. Chem. Phys.* **28** (1958) 1262.
13. T. J. ROWLAND, "Nuclear Magnetic Resonance in Metals" (Pergamon Press, Oxford), (Russian translation, Izd. Metalurgia Moskva 1964, p. 73).
14. L. STĂNESCU, E. INDREA, I. ARDELEARE, M. COLDEA, I. BRATU and D. STĂNESCU, *Rev. Roum. Phys.* **21** (1976) 939.

15. E. BURZO, L. STĂNESCU and D. UNGUR, *Sol. State Comm.* **18** (1976) 537.
16. R. J. D. TILLEY and B. G. HYDE, *J. Phys. Chem. Solids* **31** (1970) 1613.
17. B. G. HYDE and R. J. D. TILLEY, *Phys. Stat Sol. (a)* **2** (1970) 749.
18. N. F. MOTT, *Adv. Phys.* **16** (1967) 49.
19. N. FRITZSCHE, *Ann, Rev. Mater. Sci.* **2** (1972) 697.
20. J. HAEMERS, E. BAENTES and J. VENNIK, *Phys. Stat. Sol. (a)* **20** (1973) 381.
21. L. STĂNESCU and I. ARDELEAN, *Rev. Roum., Phys.* **21** (1976) 1049.

Received 18 October and accepted 14 November 1977.